

Predictive Doping and Thickness Analysis of a Multi-Wafer SiC Warm-Wall Epi Reactor for Improved Layer Cpk

Muhammad Ali Johar^{1,a}, Kanwar Singh^{2,b} and Albert Augustus Burk Jr^{3,c}

Coherent Corp. 2251 Newlins Mill Rd. Easton, PA USA 18045

^amuhammadali.johar@coherent.com, ^bKanwar.singh@coherent.com, ^calbert.burk@coherent.com

Keywords: 4H-SiC, Epitaxy, Predictive doping, predictive thickness, Cpk, MOCVD, multi-wafer reactor, Si/C ratio.

Abstract. Rapid progress in the growth of 4H-SiC epitaxial layers allow device scientists/engineers to tighten the specifications of doping and thickness uniformities of SiC epitaxial films. Further, reducing the cost of SiC epitaxial layers is a continuing goal. A compelling approach is to choose a multi-wafer warm-wall epi reactor which has been shown to have very high wafer throughput. The precursors decompose upon heating by passing over hot reactor components, however, the precursor molecules crack before reaching the substrate and can form parasitic SiC coatings. Such coatings change the emissivity of reactor parts, changing their temperatures. The allowed vapor pressure in the gas phase is also a function of the chemical composition of these deposits. Consequently, the effective Si/C ratio at the wafer varies the nitrogen incorporation efficiency on the SiC epitaxial wafer. In this paper, we have reported an approach on how to minimize the effect of changing Si/C ratio on absolute layer doping and thickness over the full campaign. We analyzed the data, identified the pattern, and have used it to make predictions or decisions to keep the deviation within control limits. The nitrogen incorporation was analyzed as a function of cumulative coating on the reactor parts. The derived models were used to make the decisions for predictive doping by adjusting the flow rates of nitrogen precursors during upcoming campaigns at specific cumulative thickness of reactor parts coating. The same approach was also used for the adjustment of growth time to obtain the targeted epi layer thickness as a function of cumulative coating. Consequently, the predictive doping control resulted in the improvement of doping Cpk from 0.37 to >1.67 and the predictive thickness control resulted in the improvement of thickness Cpk from 0.75 to 1.61. This implies that the process is six sigma qualified and expected overall nonconformance was 0.001% for doping. Moreover, the average 200 source contrast projected 5×5 mm² chip yield using a Lasertec system 88-HIT and the machine learning based PLDLZ recipe was >94% by considering the Particle, Bump, Micropipe, ComplexSF, Polytype Inclusion, Particle Inclusion, and ScratchTrace as device killer defects. The average BPDs were <25 on 150mm wafers using a 1μm thick buffer layer. Initial results on 200 mm wafers are also presented.

Introduction

The demand of electric vehicles has increased significantly over the last 5 years resulting in high demand of power electronic components such as MOSFETs, Schottky, and JBS diodes [1–5]. Silicon carbide (SiC) is outperforming other materials (Si and III-Nitrides) for high power electronic applications because of excellent physical, chemical, electrical, and thermal properties such as better thermal conductivity, low thermal expansion and excellent thermal shock resistance, low power and switching losses, high energy conversion efficiency, high operating frequency, high operating temperature, small die size for same power, long lifetime, and possibility of excellent thermal management. Further, the benefits include significant efficiency gains through miniaturization advancements, decreased cooling requirement with reduced cost. Within the last decade, high quality 150 mm SiC substrates have become available which, when combined with 150 mm epitaxy should further drive cost reduction, and multiwafer epi reactor serves the purpose of reducing the cost [6].

Over the last few years, the same effort is being implemented on 200 mm substrates and epitaxy to reduce the cost using multiwafer chemical vapor deposition (CVD).

In a typical warm wall or hot wall CVD reactor, the precursors of SiC are heated before reaching the substrate. As a result of the high temperature, the precursors decompose before reaching the substrate, and form the compounds which deposit on the reactor parts upstream, called parasitic deposits. The parasitic deposits are not 2D in geometry and are polycrystalline in nature, having a variety of textures. It is well known that the vapor pressure of material is function of the surface, this means that the vapor pressure of silicon and carbon precursors vary as a function of the coating on upstream reactor parts and local temperature, ultimately changing the vapor pressure leads to variation in decomposition of precursors which results in variation in Si/C carbon ratio. The nitrogen incorporation efficiency follows the trend of multi order polynomial as function of Si/C ratio [7]. Such variation in doping needs to be adjusted proactively by developing a statistical predictive model to achieve the desired doping in the epitaxial layer. These models help to predict the change in doping as function of cumulative coating on the reactor parts.

Experimental Methods

To grow the epitaxial layer, double side polished N-type 4H-SiC substrates with 4° off-axis cut angle towards $[11\bar{2}0]$ were used. The diameter of the substrates was 150mm and 200mm. A multiwafer CVD tool was used to grow the epitaxial layer atop substrates. The precursors for Si, C, and Cl were trichlorosilane (HCl_3Si), ethylene (C_2H_4), and hydrochloric acid (HCl), respectively. For the characterization of epitaxial films, FTIR was used to measure the thickness, Corona charge CV (CnCV) was used to measure the doping using non-contact mode, and the defectivity was evaluated by lasertech system 88-HIT. In total, 400 plus epi wafers were grown to analyze the doping incorporation efficiency versus cumulative coating. To summarize the data, Microsoft excel was used with JMP17 to analyze the data fitting the curves to get the trends of doping incorporation efficiency and growth rates as function of cumulative coating on reactor parts.

Results and Discussions

The thickness target of epitaxially grown wafers was $10.7\mu\text{m}$ and the doping target was $9.5 \times 10^{15} \text{cm}^{-3}$. The thickness reduced from 10.71 to 9.95 as function of cumulative coating as shown in Fig.1(a)

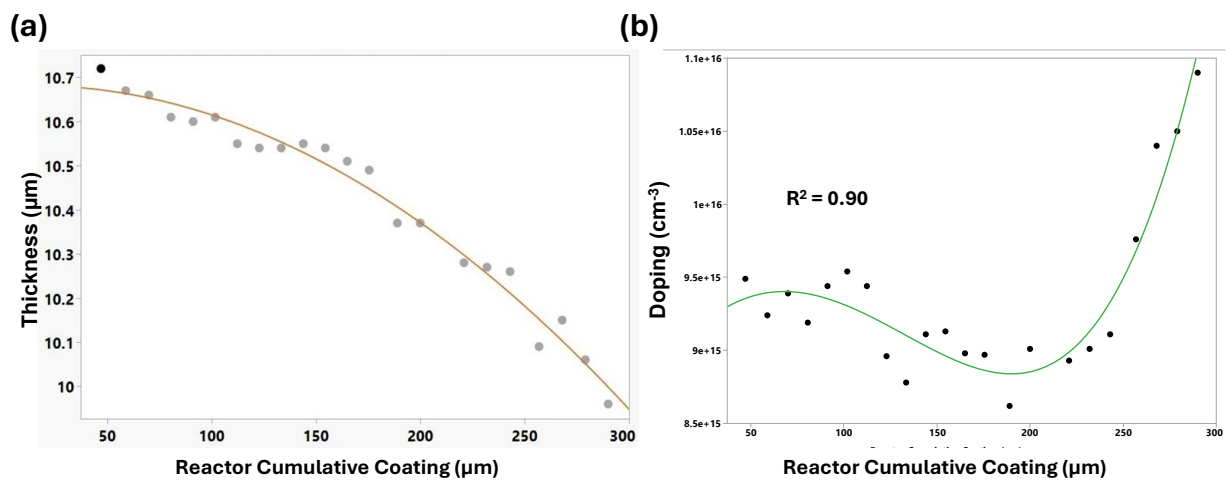


Fig. 1. (a) Average thickness and (b) average doping as function of cumulative coating of multi-wafer reactor without any adjustment for full campaign before PM.

The goodness of the fit (R^2) was 0.976. The 2nd order polynomial equation for thickness change over cumulative coating is given in eq. (1)

$$T_p = T_t - a_1 \cdot T_c - a_2(T_c - T_{cr})^2 \quad (1)$$

Where, “ T_p ” is predicted thickness of the film, “ T_t ” is the target thickness of the film, “ a_1 ” and “ a_2 ” are the constants which remain constant for one reactor type and will change based on reactor design, growth rate, growth temperature, and growth pressure. “ T_c ” is the cumulative thickness of the reactor parts. “ T_{cr} ” is the limit of the critical cumulative thickness used in the 2nd order polynomial part of the equation only

For doping, the target was $9.5 \times 10^{15} \text{cm}^{-3}$ and the effect of cumulative coating on doping is shown in Fig.1(b). The doping increased as high as $1.1 \times 10^{16} \text{cm}^{-3}$ without any adjustment. The 4th order polynomial equation to get the predicted doping as a function of cumulative equation is shown in eq. (2). The goodness of fit (R^2) was 0.90 for the fit of doping trend.

$$N_p = N_t + c_1 \times T_c + c_2(T_c - T_{cr})^2 + c_3(T_c - T_{cr})^3 \quad (2)$$

Where, “ N_p ” is the predicted doping. “ N_t ” is the target doping. “ c_1 ”, “ c_2 ”, and “ c_3 ” are the constants for one reactor type and will change based on reactor design, growth rate, growth temperature, and growth pressure.

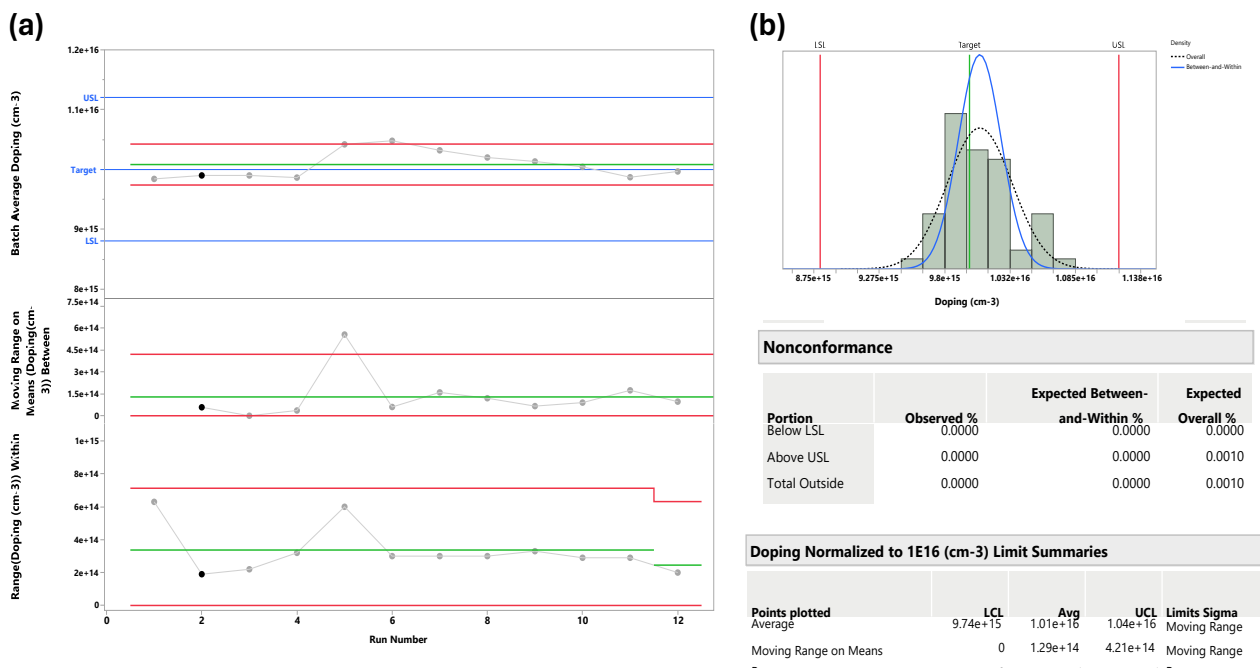


Fig. 2. (a) Three-way control chart of doping for full campaign (300μm) and (b) process capability analysis histogram, nonconformance, and doping control limits.

Following the early campaigns, the developed models shown in eq. (1) and eq. (2) were implemented and the thickness and doping were achieved very close to target. For further analysis, the Cpk were also calculated, and the predictive thickness control resulted in the improvement of thickness Cpk from 0.75 to 1.61, and the improvement of doping Cpk was observed from 0.37 to >1.67. This approach helped us to make our process six sigma qualified. The standard process control (SPC) charts of doping are shown in Figs2(a) & 2(b) with target doping of $1.0 \times 10^{16} \text{cm}^{-3}$. The average doping of the multi epi wafers grown in a single run was barely found outside the control limits as depicted from the Fig.2(a). The average moving range on means was $1.29 \times 10^{14} \text{cm}^{-3}$ with upper control limit of $4.21 \times 10^{14} \text{cm}^{-3}$. The average doping of the full campaign was $1.01 \times 10^{16} \text{cm}^{-3}$ (target was

$1.0 \times 10^{16} \text{cm}^{-3}$) with lower control limit (LCL) and upper control limit (UCL) of $9.74 \times 10^{15} \text{cm}^{-3}$, $1.04 \times 10^{16} \text{cm}^{-3}$, respectively, which are within the upper specification limit (USL) ($1.12 \times 10^{16} \text{cm}^{-3}$) and lower specification limit (LSL) ($8.80 \times 10^{15} \text{cm}^{-3}$). The Nonconformance of the process was observed as 0.0010%.

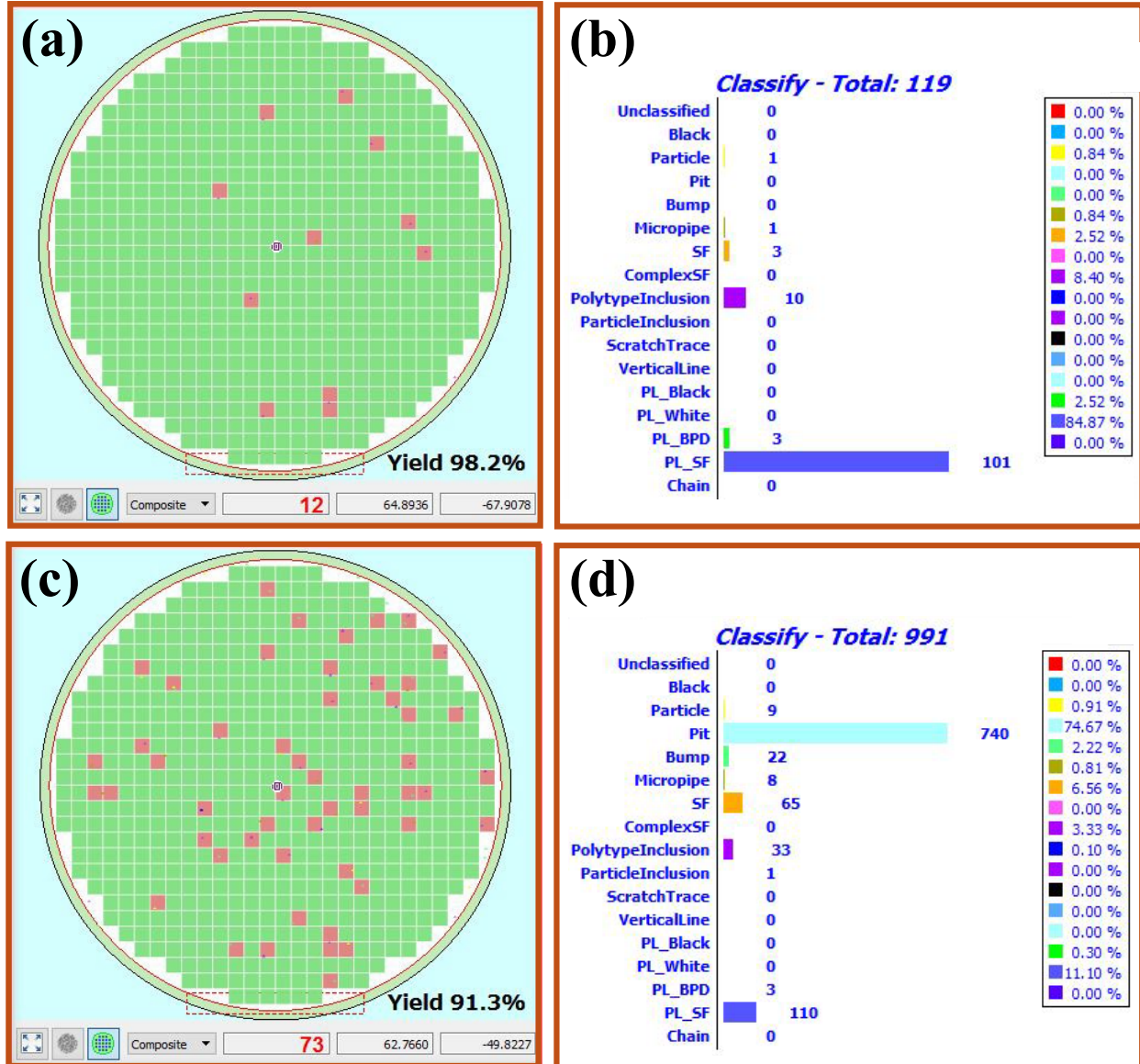


Fig. 3. $5 \times 5 \text{mm}^2$ Chip Yield by LT SICA, Coherent chosen device killer defects: Particle, Bump, Micropipe, ComplexSF, Polytype Inclusion, Particle Inclusion, and ScratchTrace: excluded non-killer-defects; Unclassified, Black, Pit, SF, Vline, PL_Black, PL_White, PL_BPD, PL_SF, Chain, (a) $5 \times 5 \text{mm}$ chip yield using 200 source contrast, (b) histogram of defects at 200 source contrast with Vlines off, (c) $5 \times 5 \text{mm}$ chip yield using 0 source contrast, and (d) histogram of defects at 0 source contrast with Vlines off.

An example of the defect evaluation of 150mm wafers used in these experiments is shown in Fig.3. Fig.3(a) shows the chip yield ($5 \times 5 \text{mm}^2$) against the device killer defects chosen by Coherent Corp. such as Particle, Bump, Micropipe, ComplexSF, Polytype Inclusion, Particle Inclusion, and ScratchTrace, which shows the chip yield of 98.2%, however, the average chip yield ($5 \times 5 \text{mm}^2$) of all epi wafers at 200 source contrast under the same criteria was 94.7% and BPDs were below 25. Fig.3(b) shows the histogram of all defects at 200 source contrast. Fig.3(c) shows the chip yield ($5 \times 5 \text{mm}^2$) against the device killer defects chosen by Coherent Corp. at 0 source contrast which is 91.3%. The histogram of all defects same map at 0 source contrast is shown in Fig.3(d).

Along with 150 mm epitaxial capability, the 200mm epitaxy current best results were 0.27% thickness uniformity, 1.1% doping uniformity, and 200 source contrast chip yield ($5 \times 5 \text{ mm}^2$) was >94%. More 200mm results will be published in upcoming papers.

Summary/Conclusions

In summary, we have developed an approach-based machine behavior to control the thickness, doping, and uniformity to increase the epi reactor yield and throughput for a multiwafer SiC epi reactor. The same process is implemented on our 150mm and 200mm epi process. Our results confirmed that our process is six sigma qualified and one can benefit from predictive doping and thickness control.

Acknowledgements

For this effort, we acknowledge the support by Coherent SiC epi process engineers (Philip Frey, Rajat Jain, Troy Tomlinson, Mark Strzelecki and Rick Vega), our SiC epi equipment team (Martin Wilcox, Brad Howsare, Steve Nemeth, and Juan Sosa), and our SiC substrate team. We gratefully acknowledge partial funding for this work under AFRL under contract number “FA8650-17-2-1727 P00015”, Jane Thompson contract monitor and Joseph Merrett technical advisor.

References

- [1] O. Seok, I.H. Kang, H.W. Kim, J.H. Moon, M. Na, S. Kim, N.K. Kim, Y.-J. Kim, H.J. Jung, W. Bahng, 1.2 kV SiC trench MOSFETs with double p-base junctions, (n.d.).
- [2] A. Kanale, T.H. Cheng, K.J. Han, B.J. Baliga, S. Bhattacharya, D. Hopkins, 1.2 kV, 10 A, 4H-SiC Bi-Directional Field Effect Transistor (BiDFET) with Low On-State Voltage Drop, Mater. Sci. Forum 1004 (2020) 872–881. <https://doi.org/10.4028/www.scientific.net/MSF.1004.872>.
- [3] A. Koyama, Y. Kiuchi, T. Mizushima, K. Takenaka, S. Matsunaga, M. Sometani, K. Nakayama, H. Ishimori, A. Kimoto, M. Takei, T. Kato, Y. Yonezawa, H. Okumura, 20 kV-Class Ultra-High Voltage 4H-SiC n-IE-IGBTs, Mater. Sci. Forum 1004 (2020) 899–904. <https://doi.org/10.4028/www.scientific.net/MSF.1004.899>.
- [4] A. Gendron-Hansen, C. Hong, Y.F. Jiang, J. May, D. Sdrulla, B. Odekirk, A.S. Kashyap, Commercialization of Highly Rugged 4H-SiC 3300 V Schottky Diodes and Power MOSFETs, Mater. Sci. Forum 1004 (2020) 822–829. <https://doi.org/10.4028/www.scientific.net/MSF.1004.822>.
- [5] D. Todo, H. Hanafusa, S. Higashi, Investigation on Electrical Characteristics of 4H-SiC Schottky-Barrier- Diodes after Silicon-Cap-Annealing, (n.d.).
- [6] A.A. Burk, D. Tsvetkov, M.J. O’Loughlin, S. Ustin, L. Garrett, A.R. Powell, J. Seaman, N. Partin, Latest SiC Epitaxial Layer Growth Results in a High-Throughput 6×150 mm Warm-Wall Planetary Reactor, Mater. Sci. Forum 778–780 (2014) 113–116. <https://doi.org/10.4028/www.scientific.net/MSF.778-780.113>.
- [7] L.B. Rowland, A.A. Burk, C.D. Brandt, Nitrogen Doping Efficiency During Vapor Phase Epitaxy of 4H-SiC, Mater. Sci. Forum 264–268 (1998) 115–118. <https://doi.org/10.4028/www.scientific.net/MSF.264-268.115>.